Advanced Models and Fast Simulation Algorithms for MARS Plants

Phani R V Marthi[1,2*], Suman Debnath[1†], Qianxue Xia[3‡], Maryam Saeedifard[3§]
[1]Oak Ridge National Laboratory, [2]Missouri University of Science and Technology, [3]Georgia Institute of Technology
Email: *marthip@ornl.gov, †debnaths@ornl.gov, ‡qxia31@gatech.edu, §maryam@ece.gatech.edu

***Abstract*—With the successful commercialization of modular multilevel converters (MMC) and rapid increase in photovoltaic (PV) penetration and energy storage systems (ESS), one of the research areas being explored dynamically is integration of PV systems and ESS systems to MMCs. On this front, an integrated development of PV plants, ESS, and alternating- and direct-current (ac/dc) systems through Multi-Port Autonomous Reconfigurable Solar (MARS) plant is proposed and being researched upon. However, simulation of MARS systems on traditional existing software takes very long time (order of days) due to the presence of a large number of states and non-linear devices. Therefore, development of fast high fidelity models is of paramount importance to test the hardware design, control design and planning of power system expansions. In this context, two research objectives are addressed in this paper: firstly, an ultra fast single- or multi- CPU simulation algorithm to simulate the MARS system based on state-space models, hybrid discretization algorithm with a relaxation technique that reduces the imposed computational burden and a multi-rate method is presented. Secondly, a reduced order model of MARS is also presented. Both the developed techniques are validated with respect to reference PSCAD/EMTDC model.**

I. Introduction

Due to their attractive features, modular multilevel converters (MMCs) and their variants such as alternate arm converters (AACs) [1] and cascaded two-level converters (CTLs) [2] have achieved commercial success in the recent years [3], [4]. The technical and economic merits of solar integrated systems (PV) and energy storage systems (ESS) have increased the installation pace of renewable sources all across United States. These two achievements have led to growing interest in research on integration of PV and ESS systems to MMCs. In this avenue, integration of PV and ESS systems through a new topology called Multi-Port Autonomous Reconfigurable Solar(MARS) plant is proposed in this paper.

MARS circuit configuration is novel and different when compared to the circuit configurations of PV- and ESS integrated MMC systems proposed in the previous research endeavors [5]–[8]. The research works in [5]–[8] look into

This manuscript has been authored by UT-Battelle, LLC under Contract No. DE-AC05-00OR22725 with the U.S. Department of Energy. The United States Government retains and the publisher, by accepting the article for publication, acknowledges that the United States Government retains a non-exclusive, paid-up, irrevocable, world-wide license to publish or reproduce the published form of this manuscript, or allow others to do so, for United States Government purposes. The Department of Energy will provide public access to these results of federally sponsored research in accordance with the DOE Public Access Plan(http://energy.gov/downloads/doe-public-access-plan).

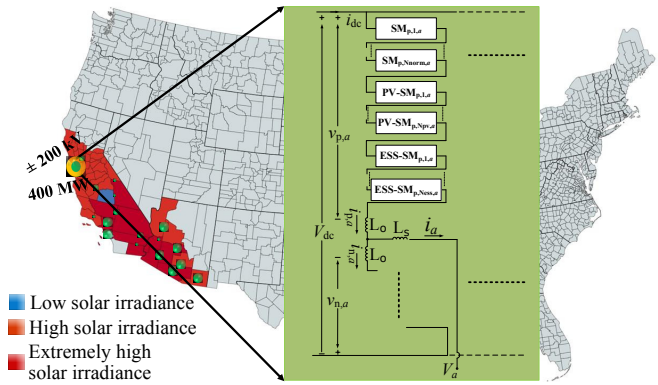

Fig. 1: Integration of MARS-HVdc system

either PV systems or BESS systems or both and do not look at more than 15 SMs per arm. In MARS, normal submodules(SMs), PV SMs and ESS SMs are co-located in an arm of a phase leg with more than 200 SMs. The total number of SMs in three phase MARS system are more than 1200 and number of states being more than 7000. Due to the presence of thousands of states and hundreds of SMs, simulation of MARS system is computationally complex and time consuming. Also, numerical stiffness is identified in MARS which add to the computational complexity and long simulation times. These issues call for a unique simulation algorithm to simulate MARS system. Therefore it is important to model and simulate MARS with an algorithm to reduce the imposed computational burdens.

In this paper, two models for fast and accurate simulation of MARS HVdc systems are presented. Firstly, a high fidelity model based on hybrid discretization and hysteresis algorithm is presented in Sections II and III. Secondly, a reduced order model based on minimal number of states is presented in Section IV.

The high-fidelity model of MARS helps with evaluating the hierarchical multi-level controllers. In reduced order model, averaged-value approach is applied to define the dynamics of ac-side currents. The states within the PV or ESS systems or the dc-side currents are neglected. The model helps tune the higher level controller. The developed models are tested on different systems and validated using reference PSCAD/EMTDC models under various operating conditions.

$$(L_o + L_s)\frac{\mathrm{d}i_{\mathrm{p},j}}{\mathrm{d}t} - L_s\frac{\mathrm{d}i_{\mathrm{n},j}}{\mathrm{d}t} = -(R_o + R_s)\, i_{\mathrm{p},j} + R_s i_{\mathrm{n},j} + \frac{V_{\mathrm{dc}}}{2} - v_j - v_{\mathrm{cm}} - v_{\mathrm{p},j}, \forall j \in (a,b,c), \tag{1a}$$

$$(L_o + L_s)\frac{\mathrm{d}i_{\mathrm{n},j}}{\mathrm{d}t} - L_s\frac{\mathrm{d}i_{\mathrm{p},j}}{\mathrm{d}t} = -(R_o + R_s)\, i_{\mathrm{n},j} + R_s i_{\mathrm{p},j} + \frac{V_{\mathrm{dc}}}{2} + v_j + v_{\mathrm{cm}} - v_{\mathrm{n},j}, \forall j \in (a,b,c), \tag{1b}$$

$$v_{\mathrm{y},j} = \sum_{\mathrm{l}=1}^{\mathrm{N_{norm}}} v_{\mathrm{smnorm,y,l},j} + \sum_{\mathrm{l}=\mathrm{N_{norm}}+1}^{\mathrm{N_{pv}}} v_{\mathrm{smpv,y,l},j} + \sum_{\mathrm{l}=\mathrm{N_{pv}}+1}^{\mathrm{N_{ess}}} v_{\mathrm{smess,y,l},j} \tag{1c}$$

$$\sum_{\mathrm{l}=\mathrm{l_x}}^{\mathrm{N_x}} v_{\mathrm{smx,y,l},j} = \sum_{\mathrm{l}=\mathrm{l_x}}^{\mathrm{N_x}} \left[S_{\mathrm{yl1},j} v_{\mathrm{cy,l},j} + \left\{(1 - S_{\mathrm{yl1},j})(1 - S_{\mathrm{yl2},j})\, v_{\mathrm{cy,l},j}\right\} \mathrm{sgn}\,(i_{\mathrm{y},j})\right], \forall \mathrm{y} \in (\mathrm{p},\mathrm{n}), \forall j \in (a,b,c) \tag{1d}$$

where,

$v_{\mathrm{smx,y,l},j} = v_{\mathrm{smnorm,y,l},j}(\mathrm{or}) v_{\mathrm{smpv,y,l},j}(\mathrm{or}) v_{\mathrm{smess,y,l},j}$;$\mathrm{l_x} = 1(\mathrm{or})(\mathrm{N_{norm}}+1)(\mathrm{or})(\mathrm{N_{pv}}+1)$;$\mathrm{N_x} = \mathrm{N_{norm}}(\mathrm{or})(\mathrm{N_{pv}})(\mathrm{or})(\mathrm{N_{ess}})$

II. High Fidelity MARS-HVDC Model

Based on solar resources and load centers, an example of MARS system integration is shown in Fig. 1. In Fig. 1, upper arm of phase a is highlighted and shown. The MARS circuit topology has three phases. Each phase $j \in (a,b,c)$ has two phase-legs, each phase-leg has two arms, and each arm $\mathrm{y} \in (\mathrm{p},\mathrm{n})$ has total "N" SMs. The SMs can be a normal half-bridge system, a half-bridge with dc-dc converter connecting to PV system, and a half-bridge with dc-dc converter connecting to energy storage. The SMs in each arm are divided into "Nnorm" normal SMs, "Npv" PV-SMs, and "Ness" number of ESS-SMs. The arm inductor is sized based on the fault current limits and the SM capacitor is determined based on capacitor voltage ripple requirements. The PV- and ESS SM inductors are sized based on the dc-dc converter inductor current ripple requirements.

The total number of states within MARS system are $(18\mathrm{N_{norm}} + 36\mathrm{N_{pv}} + 42\mathrm{N_{ess}})$ + 6. These states include the arm currents, normal SM capacitor voltages, PV-SM capacitor voltages, PV-SM inductor currents, ESS-SM capacitor voltages, ESS-SM inductor currents, and semiconductor switching states ($S_{\mathrm{ylx},j}$). The arm current dynamics are given in (1). The comprehensive description of other terms in (1) and normal SMs' operation is detailed in [9] and [10].

A. PV SM

The PV system is integrated into an SM using a boost converter. The inductor current (i_{Lpv}) dynamics in the boost converter are given by (2).

$$L_{\mathrm{pv}}\frac{\mathrm{d}i_{\mathrm{Lpv,y,l},j}}{\mathrm{d}t} = v_{\mathrm{cpv,y,l},j} - (1 - S_{\mathrm{yl3},j})\, v_{\mathrm{c,y,l},j} \times \mathrm{sgn}\,(i_{\mathrm{Lpv,y,l},j}) \tag{2}$$

The dynamics of SM capacitor voltages $(v_{\mathrm{c,y,l},j})$ in PV-SM are given by (3).

$$C_{\mathrm{SM}}\frac{\mathrm{d}v_{\mathrm{c,y,l},j}}{\mathrm{d}t} = -\frac{v_{\mathrm{c,y,l},j}}{R_p} - i_{\mathrm{y,l},j} + (1 - S_{\mathrm{yl3},j}) \times (i_{\mathrm{Lpv,y,l},j}.\mathrm{sgn}\,(i_{\mathrm{Lpv,y,l},j})) \tag{3}$$

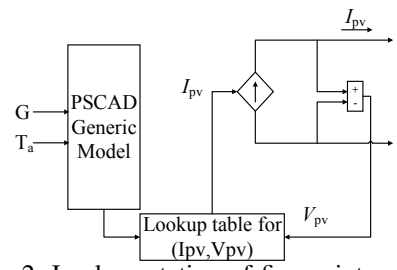

Fig. 2: Implementation of five-point model

where,

$$i_{\mathrm{y,l},j} = -S_{\mathrm{yl1},j} i_{\mathrm{y},j} - (1 - S_{\mathrm{yl1},j})(1 - S_{\mathrm{yl2},j})\,\mathrm{sgn}\,(i_{\mathrm{y},j})$$

The PV input capacitor dynamics $(v_{\mathrm{cpv,y,l},j})$ are given by (4)

$$C_{\mathrm{pv}}\frac{\mathrm{d}v_{\mathrm{cpv,y,l},j}}{\mathrm{d}t} = i_{\mathrm{pv,y,l},j} - i_{\mathrm{Lpv,y,l},j} \tag{4}$$

B. ESS SM

The ESS system is integrated into the SM using a bidirectional dc-dc converter. The inductor current (i_{Less}) dynamics in the bi-directional converter are given in (5).

$$L_{\mathrm{ess}}\frac{\mathrm{d}i_{\mathrm{Less,y,l},j}}{\mathrm{d}t} = v_{\mathrm{cess,y,l},j} - S_{\mathrm{yl4},j}(1 - S_{\mathrm{yl3},j})\, v_{\mathrm{c,y,l},j} \times (1 - S_{\mathrm{yi3},j})(1 - S_{\mathrm{yi4},j})\, v_{\mathrm{cyi},j}\mathrm{sgn}\,(i_{\mathrm{Less,y,l},j}) \tag{5}$$

The dynamics of SM capacitor voltages in ESS-SM are given by (6).

$$C_{\mathrm{SM}}\frac{\mathrm{d}v_{\mathrm{c,y,l},j}}{\mathrm{d}t} = -\frac{v_{\mathrm{c,y,l},j}}{R_p} - i_{\mathrm{y,l},j} + S_{\mathrm{yl4},j}(1 - S_{\mathrm{yl3},j})\, i_{\mathrm{Less,y,l},j} + (1 - S_{\mathrm{yl4},j})(1 - S_{\mathrm{yl3},j}) \times (i_{\mathrm{Less,y,l},j}.\mathrm{sgn}\,(i_{\mathrm{Less,y,l},j})) \tag{6}$$

The ESS input capacitor dynamics $(v_{\mathrm{cess,y,l},j})$ are given by (7)

$$C_{\mathrm{ess}}\frac{\mathrm{d}v_{\mathrm{cess,y,l},j}}{\mathrm{d}t} = i_{\mathrm{ess,y,l},j} - i_{\mathrm{Less,y,l},j} \tag{7}$$

C. PV and ESS Models

Single diode PV model [11] is computationally very expensive to implement in real-time simulation studies. This arises from the presence of exponential term in diode current of current voltage equation. To reduce the computational burden, a five-point PV model based on simulation and empirical data is developed and validated with generic PV model in PSCAD. The idea of this model is to generate a look-up table that outputs the current generated from PV (i_{pv}) based on the variation of voltage measured at PV terminals (v_{pv}). The five-point model contains five points in the i_{pv}-v_{pv} curve obtained from the PV panel datasheet. The five points are (0, I_{sc}), (V_{mp}, I_{mp}), (V_{oc}/2, i_3), ((V_{oc}+V_{mp})/2, i_4), and (0, V_{oc}). The terms i_3 and i_4 are obtained from i_{pv}-v_{pv} curves. The rest of the currents are obtained from extrapolating these known points. Based on these extrapolated curves, i_{pv} is generated which feeds into the dc-dc converter. The implementation is summarized in Fig. 2.

The ESS model consists of a voltage source Eb and an internal series resistance Rbatt. In this model, the battery's state of charge (SOC) is considered [11].

III. Simulation Algorithm for High-Fidelity MARS model

MARS system can be represented as a non-linear non-autonomous switched system and derived as a system of semi-explicit differential algebraic equations (DAEs). The so derived high-fidelity model of MARS is partitioned based on the numerical stiffness associated with the states and then the seperated states are discretized using the hybrid discretization method described in [9].

Numerical stiffness is observed in arm currents and inductor currents dynamics of both PV and ESS SMs under blocked condition scenario. This is due to the presence of the sgn function in (1). In the capacitor voltages' dynamics numerical stiffness is not observed, as the sgn function present in them is treated as an external input.

The SM capacitor voltages' dynamics, and PV and ESS input capacitor dynamics are discretized using forward Euler, which is a non-stiff explicit discretization algorithm. Implicit discretization algorithms with stiff-decay and A-stable properties such as backward Euler are used to discretize the arm current dynamics and inductor current dynamics. In comparison to conventional simulation of MARS system, hybrid discretization-based simulation reduces the matrix size to 5 × 5 from (6($\mathrm{N_{norm}}+\mathrm{N_{pv}}+\mathrm{N_{ess}}$) + 5) × (6($\mathrm{N_{norm}}+\mathrm{N_{pv}}+\mathrm{N_{ess}}$) + 5). In addition to the whole system matrix size reduction, the matrix size reduction in the dc-dc converter is also observed. If hybrid discretization is applied like in [9] alone, PV- and ESS-dc-dc converters will require 6($\mathrm{N_{pv}}+\mathrm{N_{ess}}$) inversions of (2×2) matrices in comparison to simple arithmetic computations of 6($\mathrm{N_{pv}}$ + $\mathrm{N_{ess}}$) equations. This results in huge reduction of computational costs as inverting a 5×5 matrix and calculating simple arithmetic equations is computationally inexpensive.

To reduce the stiffness in the PV and ESS SMs, a hysteresis relaxation technique is introduced that approximates

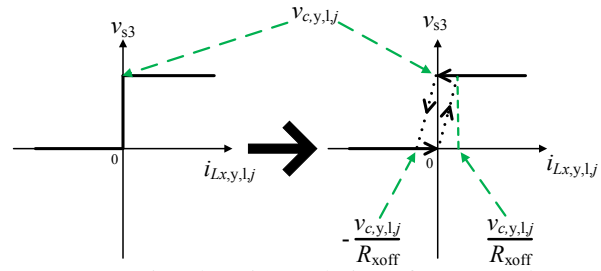

Fig. 3: Hysteresis relaxation technique for PV- and ESS-SM

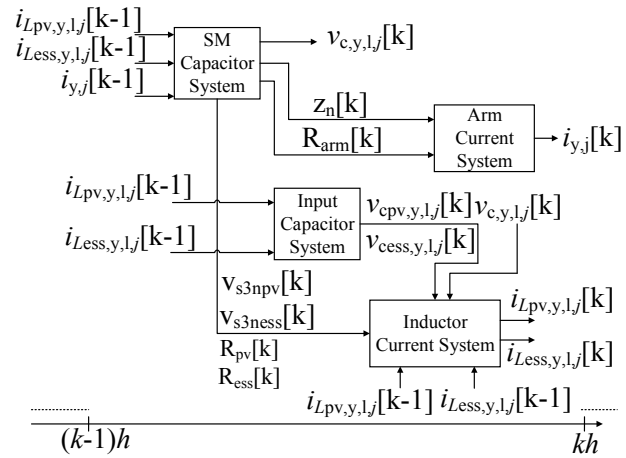

Fig. 4: Detailed implementation of the MARS-HVdc simulation

the voltage across the switches in the dc-dc converters of PV and ESS SMs.The proposed hysteresis relaxation technique is shown in Fig. 3. In the case of PV- and ESS SM, the modified voltage across dc-dc converter switch under blocked operating condition is implemented as follows:

$$\tilde{v}_{\mathrm{s3}}[k] = v_{\mathrm{s3nx,y,l},j}[k] + i_{\mathrm{Lx,y,l},j}[k]R_{\mathrm{x,y,l},j}[k], \tag{8}$$

where $v_{\mathrm{s3nx,y,l},j}[k]$, $i_{\mathrm{Lx,y,l},j}[k]$ and $R_{\mathrm{x,y,l},j}[k]$ are defined in (9). The detailed implementation of MARS-HVdc simulation algorithm is summarized in Fig. 4.

IV. Reduced-Order Model

The block diagram of the reduced-order model of MARS system is shown in Fig. 5, with the assumption of balancing SM capacitor voltages (V_{smnorm}, V_{smpv}, and V_{smess})with negligible ripple. It is worth noting that $\mathrm{m_i^u}$ and $\mathrm{m_i^l}$, i = 1, 2, 3 are the modulation indexes for normal-, PV- and ESS-SMs, which are computed by the controller. The reduced-order model of MARS consists of the equivalent model of hardware as shown in Fig. 6 and the upper-level controller. In the equivalent model of MARS hardware, the voltage in each arm is averaged to remove the switching dynamics in (1). The voltage in each arm is modelled using an externally controlled voltage source, with the external input signal dependent on the upper-level controller. In this model, the capacitor voltages of all the SMs in the arms are assumed to be balanced and the same. The reduced-order model of MARS is controlled to generate

$$v_{\mathrm{s3nx,y,l},j}[k] = \begin{cases} 0, & \text{if} \quad \left(\quad i_{\mathrm{Lx,y,l},j}[k-2] < 0 \quad \text{and} \quad i_{\mathrm{Lx,y,l},j}[k-1] < -\dfrac{v_{\mathrm{c,y,l},j}[k]}{R_{\mathrm{xoff}}} \right), \\ 0, & \text{if} \quad (i_{\mathrm{Lx,y,l},j}[k-2] < 0 \quad \text{and} \quad i_{\mathrm{Lx,y,l},j}[k-1] > 0) \quad \text{or} \quad \left(0 < i_{\mathrm{Lx,y,l},j}[k-1] < \dfrac{v_{\mathrm{c,y,l},j}[k]}{R_{\mathrm{xoff}}} \right), \\ v_{\mathrm{c,y,l},j}[k], & \text{otherwise.} \end{cases} \tag{9a}$$

$$R_{\mathrm{x,y,l},j}[k] = \begin{cases} 0, & \text{if} \quad \left(i_{\mathrm{Lx,y,l},j}[k-2] < 0 \quad \text{and} \quad i_{\mathrm{Lx,y,l},j}[k-1] < -\dfrac{v_{\mathrm{c,y,l},j}[k]}{R_{\mathrm{xoff}}} \right), \\ 0, & \text{if} \quad \left(i_{\mathrm{Lx,y,l},j}[k-2] > 0 \quad \text{and} \quad i_{\mathrm{Lx,y,l},j}[k-1] > \dfrac{v_{\mathrm{c,y,l},j}[k]}{R_{\mathrm{xoff}}} \right), \\ R_{\mathrm{xoff}}, & \text{otherwise.} \end{cases} \tag{9b}$$

$$\text{where,} \quad i_{\mathrm{Lx,y,l},j} = i_{\mathrm{Lpv,y,l},j}(\mathrm{or}) i_{\mathrm{Less,y,l},j}; R_{\mathrm{xoff}} = R_{\mathrm{pvoff}}(\mathrm{or}) R_{\mathrm{essoff}}; v_{\mathrm{s3nx,y,l},j} = v_{\mathrm{s3npv,y,l},j}(\mathrm{or}) v_{\mathrm{s3ness,y,l},j}$$

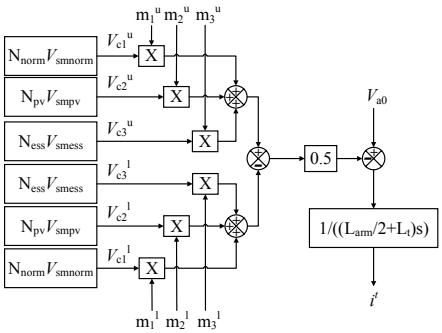

Fig. 5: Block diagram of reduced-order model for one phase of MARS system

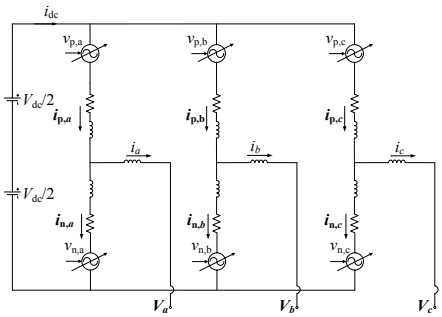

Fig. 6: Schematic of reduced-order model

dispatched active and reactive powers into the grid. The upper-level controller takes power commands as inputs to control the ac-side currents in MARS and power commands being the function of dispatch commands. Based on the available PV- and ESS power ratings, and MARS system real and reactive power ratings, maximum and minimum power limits are imposed on the upper-level controller.

V. Simulation Results & Validation

The proposed algorithm is tested on two MARS systems. The first test system is a hypothetical 50 SM MARS system used to expedite the validation process of MARS system on PSCAD platform. The test system consists of 14 normal SMs, 26 PV SMs and 10 ESS SMs. The second test system is benchmarked based on Trans Bay Cable project in Pittsburg, California [12]. Assuming 150 kW, 1 kV PV and ESS sub-modules (SMs), the number of each type of SM required in Pittsburg MARS are tabulated in Table I. The size of PV and ESS SMs are determined based on utilizing 200 A, 3.3 kV SiC devices.

TABLE I: Pittsburg MARS system parameters

Parameter	Value
System rating	400 MW
dc bus voltage (V_{dc})	$\pm$200 kV
ac side voltage (V_{ac})	220 kV
PV system power rating (P_{PV})	100 MW
ESS system power rating (P_{ESS})	32.8 MW
Number of normal SMs per arm (N_{norm})	102
Number of PV SMs per arm (N_{PV})	111
Number of ESS SMs per arm (N_{ESS})	37
Total number of SMs per arm (N)	250
Arm inductance (L_{o})	30.0 mH
Arm resistance (R_{o})	0.1 Ω
Grid side inductance (L_{s})	40.0 mH
Grid side resistance (R_{s})	0.83333 Ω
SM capacitor voltage (V_{SM})	1.6 kV
SM capacitance	7.7 mF

TABLE II: Summary of simulation results

Parameter	50 SM MARS system	Pittsburg MARS system
Simulation time	0.15 (secs)	0.05 (secs)
PSCAD reference	3 (hours)	48 (hours) approx.
Developed algorithm	5 (secs)	10 (secs)
Improvement	2000x approx.	17000x approx.

The following case studies are considered to compare the results obtained from the proposed simulation algorithm with the reference results : (i) with PV and ESS system sending power into the ac grid (discharging) (PV + ESS) and (ii) with PV system and ESS system receiving (charging) (PV + ESSr). The corresponding results are shown in Fig. 7 for 50 SM MARS system. The total simulation time is 0.15 secs with a step change in reference ac power at 0.1 secs. The developed model simulation results are promising in comparision to

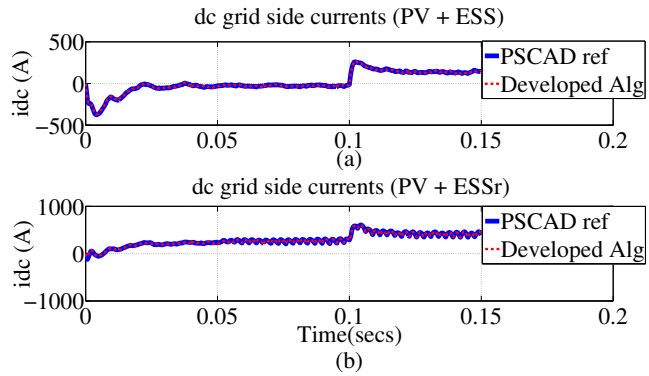

Fig. 7: (a) dc side grid currents for PV + ESS case, and (b) PV + ESSr case for 50 SM MARS system

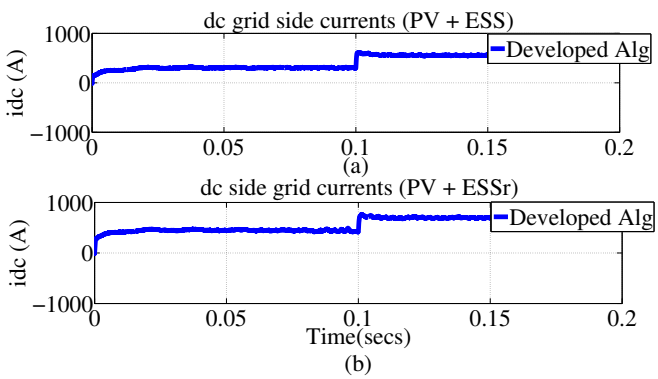

Fig. 8: (a) dc side grid currents for PV + ESS case, and (b) PV + ESSr case in MARS Pittsburg system

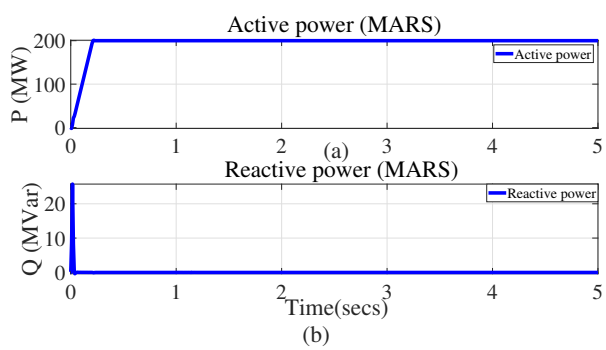

Fig. 9: Powers measured from the MARS reduced order model ac terminal: (a)active power, and (b)reactive power

reference PSCAD models with an average weighted error to be less than 2%. The results for Pittsburg MARS system with developed algorithm are shown in Fig. 8 for 0.15 secs with a step change in ac reference power at 0.1 secs. The summary of simulation results are tabulated in Table II. The reduced-order model of MARS is evaluated for given power references, and the corresponding results are shown in Fig. 9. The results indicate the stability of the reduced-order model.

VI. Conclusion

Two advanced and fast simulation models are developed in this paper for MARS systems. First, high-fidelity model is developed based on using hybrid discretization and hysteresis relaxation algorithms. Second, a reduced-order model is developed based on reduced number of states. The developed simulation models are computationally very economic, therefore will be great resources in control, design, and planning of MARS-HVdc systems. Improvements in simulation speeds of upto 17000x was observed with accuracy of more than 99%. High fidelity and reduced order MARS models are tested for different MARS systems and validated on PSCAD/EMTDC.

Acknowledgement

This paper is based upon work supported by the U.S. Department of Energy's Office of Energy Efficiency and Renewable Energy (EERE) under Solar Energy Technologies Office (SETO) Agreement Number 34019. The authors acknowledge Dr. Jiuping Pan from ABB and Dr. Sudipta Chakraborty from Opal-RT for their valuable inputs in this work. Authors would also like to thank Dr. Jian Fu and Dr. Hariharan Krishnaswami from SETO for overseeing the project developments and providing guidance. This research used resources of the National Transportation Research Center, which is a DOE Office of Science User Facility operated by the Oak Ridge National Laboratory.

References

[1] M. M. Merlin, T. C. Green, P. D. Mitcheson, D. R. Trainer, R. Critchley, W. Crookes, and F. Hassan, "The alternate arm converter: A new hybrid multilevel converter with dc-fault blocking capability," vol. 29, pp. 310–317, IEEE, 2013.

[2] B. Jacobsson, P. Karlsson, G. Asplund, L. Harnefors, and T. Jonsson, "Vsc-hvdc transmission with cascaded two-level converters," in *CIGRE Session*, pp. B4–B110, 2010.

[3] S. Du, A. Dekka, B. Wu, and N. Zargari, *Modular Multilevel Converters: Analysis, Control, and Applications*. IEEE, 2018.

[4] S. Debnath, J. Qin, B. Bahrani, M. Saeedifard, and P. Barbosa, "Operation, control, and applications of the modular multilevel converter: A review," *IEEE Transactions on Power Electronics*, vol. 30, pp. 37–53, Jan 2015.

[5] M. Vasiladiotis and A. Rufer, "Analysis and control of modular multilevel converters with integrated battery energy storage," *IEEE Transactions on Power Electronics*, vol. 30, pp. 163–175, Jan 2015.

[6] M. A. Perez, D. Arancibia, S. Kouro, and J. Rodriguez, "Modular multilevel converter with integrated storage for solar photovoltaic applications," in *IECON 2013 - 39th Annual Conference of the IEEE Industrial Electronics Society*, pp. 6993–6998, Nov 2013.

[7] H. Bayat and A. Yazdani, "A hybrid mmc-based photovoltaic and battery energy storage system," *IEEE Power and Energy Technology Systems Journal*, vol. 6, pp. 32–40, March 2019.

[8] J. Khazaei, G. Pavlak, B. Lee, and M. Elsenbaty, "A novel application of modular multi-level converters for partially shaded pv systems," in *2019 IEEE Texas Power and Energy Conference (TPEC)*, pp. 1–6, Feb 2019.

[9] S. Debnath and M. Chinthavali, "Numerical-stiffness-based simulation of mixed transmission systems," *IEEE Transactions on Industrial Electronics*, vol. 65, pp. 9215–9224, Dec 2018.

[10] S. Debnath and M. Chinthavali, "Mmc-hvdc: Simulation and control system," in *2016 IEEE Energy Conversion Congress and Exposition (ECCE)*, pp. 1–8, Sept 2016.

[11] D. Rekioua and E. Matagne, *Optimization of Photovoltaic Power Systems*. Springer, 2012.

[12] H. Knaak, "Modular multilevel converters and hvdc/facts: A success story," in *Proceedings of the 2011 14th European Conference on Power Electronics and Applications*, pp. 1–6, Aug 2011.